

Transition from sub-Poissonian to super-Poissonian shot noise in resonant quantum wells

Ya. M. Blanter and M. Büttiker

Département de Physique Théorique, Université de Genève, CH-1211, Genève 4, Switzerland
(August 11, 2021)

We investigate the transition from sub-Poissonian to super-Poissonian values of the zero-temperature shot noise power of a resonant double barrier of macroscopic cross-section. This transition occurs for driving voltages which are sufficiently strong to bring the system near an instability threshold. It is shown that interactions in combination with the energy dependence of the tunneling rates dramatically affect the noise level in such a system. Interaction-induced fluctuations of the band bottom of the well contribute to the noise and lead to a new energy in the Fano factor. They can enhance the noise to super-Poissonian values in a voltage range preceding the instability threshold of the system. At low voltages, interactions may either enhance or suppress the noise compared to the the non-interacting case.

PACS numbers: 73.50.Td, 73.23.-b, 73.20.Dx, 73.61.-r

I. INTRODUCTION

The investigation of the current noise properties provides an important tool to gain additional information on electric systems. A standard measure of the noise is the Fano factor F which is defined as the ratio of the current noise spectral density $S_I(\omega)$ and the full Poisson noise $2e\langle I \rangle$ where $\langle I \rangle$ is the average current driven through the well. Thus the Fano factor $F = S_I(\omega)/2e\langle I \rangle$ is smaller than one for sub-Poissonian noise and exceeds one for super-Poissonian noise. In this work we present theoretical results for the Fano factor of a resonant double barrier with the macroscopic cross-section and investigate the transition from *sub*-Poissonian noise to *super*-Poissonian noise.

An early experiment of Li *et al*¹ focused on the suppression of the noise power below the Poisson value. Already in this work it was noticed that the Fano factor increases from the suppressed values in the voltage range of positive differential conductance (PDC) as the range of negative differential conductance (NDC) is approached. Experiments by Brown² and Iannaccone *et al*³ showed that in the NDC range, the current noise increases even above the Poisson value, and is thus described by a Fano factor exceeding one. Recently, Kuznetsov *et al*⁴ have presented a detailed investigation of the noise oscillations from sub-Poissonian to super-Poissonian values of a resonant quantum well in the presence of a parallel magnetic field. The magnetic field leads to multiple voltage ranges of NDC and permits a clear demonstration of the effect. Below we present a theory which describes the transition from sub-Poissonian ($F < 1$) to super-Poissonian noise ($F > 1$).

Our approach treats the fluctuations of the potential and the charge in the well. The theory describes the transition from sub-Poissonian noise to super-Poissonian noise at large voltages. At smaller voltages it gives either an additional suppression of the noise power or an

enhancement of the noise power compared to theories which neglect the potential fluctuations. We find that a new quantity, an energy Λ , enters the Fano factor. The energy Λ is a measure of the sensitivity of the noise to a collective charge and current response generated by the Coulomb interaction. The interaction energy Λ is determined by the response of the average current $\langle I \rangle$ to a variation of the electrostatic potential U in the well

$$J \equiv \frac{\partial \langle I \rangle}{\partial U} \quad (1)$$

and by the response of the charge

$$C_0 \equiv -\frac{\partial \langle Q \rangle}{\partial U} \quad (2)$$

to the potential in the well. C_0 has the dimension of capacitance. It is positive in the PDC range, giving rise to screening of excess charges, and becomes negative as the NDC range is approached, corresponding to *overscreening* of excess charges. For a double barrier with a geometrical capacitance C_L across the left barrier and a geometrical capacitance C_R across the right barrier we find an interaction energy

$$\Lambda \equiv \frac{\hbar J}{C_L + C_R + C_0}. \quad (3)$$

Note that J has the dimension of a conductance. The interaction energy thus has the form of a dimensionless conductance $\hbar J/e^2$ multiplied by an effective charging energy of the well $e^2/(C_L + C_R + C_0)$. In the NDC range the charging energy grows and leads to a very large interaction energy Λ . For a resonant level characterized by decay widths $\Gamma_{L,R}$ through the left and right barrier, an asymmetry $\Delta\Gamma = (\Gamma_L - \Gamma_R)/2$, and a total width $\Gamma = \Gamma_L + \Gamma_R$, we find a Fano factor given by

$$F = \frac{1}{2} + 2\frac{(\Lambda - \Delta\Gamma)^2}{\Gamma^2}. \quad (4)$$

Note that the escape rates $\Gamma_{L,R}$ are positive quantities but Λ and $\Delta\Gamma$ can have either sign. For a symmetric double barrier the sign of $\Delta\Gamma$ is independent of the applied voltage. However, as will be shown in this work, for any barrier Λ changes sign as a function of voltage: It is negative in the stable part of the I-V-characteristic and becomes positive and large in the NDC part of the I-V characteristic.

If Λ is set to zero in Eq. (4), the Fano factor for non-interacting electrons of Chen and Ting⁵ is recovered. This result is a consequence of partition noise: an electron scattered at an obstacle with transmission probability T can only be either transmitted or reflected. The partition noise⁶⁻⁸ gives rise to shot noise proportional to $T(1-T)$. For a resonant tunneling barrier⁹, using the Breit-Wigner expression for the transmission probability, this leads immediately to the Fano factor, Eq. (4) with $\Lambda = 0$. For $\Lambda = 0$ the Fano factor is minimal (equal to $F = 1/2$) if the two barriers lead to equal escape rates $\Delta\Gamma = 0$ and the Fano factor is maximal (with a value of $F = 1$), if the double barrier structure is very asymmetric, $|\Delta\Gamma| \simeq \Gamma/2$. The lower limit $F = 1/2$ is obtained, independent of whether transmission is a quantum mechanical, fully coherent process or a sequential two step process without phase coherence¹⁰⁻¹⁴. This maximal suppression is also obtained in the presence of a magnetic field (see Ref. 15). On the other hand, models with internal degrees of freedom¹⁶ can give rise to a noise suppression slightly below $F = 1/2$, if the internal degrees of freedom couple also to the reservoirs.

Our result, Eq. (4), also has a Fano factor of $1/2$ as a lower limit. However, depending on the asymmetry, at low voltages our theory predicts either a reduction or enhancement of the Fano factor compared to a free-electron theory. A negative Λ arises if an increase of the internal voltage U decreases the current through the well. This is the case in the stable range of the I-V characteristic: a charging of the well is counteracted by the Coulomb interaction which creates a positive potential response which in turn drives the resonant level further up in energy. This leads to a Coulomb induced correction of the Fano factor for a resonant double well even at low voltages.

As the range of the NDC is approached, the interaction energy Λ changes sign and becomes positive to such a degree that it completely dominates the Fano factor. This large increase is again due to the Coulomb interaction. However, now we are in a range where the average charge increases in response to a positive variation of the internal voltage. A charge injected into the well creates a fluctuation of the internal potential which causes even more charge to flow into the well. Thus the current fluctuations are magnified and give rise to a Fano factor which exceeds the Poisson value.

Large fluctuations are commonly expected near equilibrium or non-equilibrium phase transitions. The analogy of the far from equilibrium current instabilities with equilibrium phase transitions was the subject of work by Pytte and Thomas¹⁷. These authors investigated the

critical slowing down of dielectric relaxation modes at a bulk current instability (Gunn effect). Subsequent work by Büttiker and Thomas¹⁸ analyzed a one band-current instability (superlattice) and discussed in addition to the dielectric relaxation modes also the modes which arise due to the coupling of the current fluctuations to the magnetic field. In this work we investigate the resonant well under the condition of complete external voltage control and take into account the electrostatic but not the magnetic part of the Coulomb interaction.

There are two theoretical works^{2,19} which also indicate Fano factors in excess of the Poisson value. However, these works do not include the partition noise. Instead, it is assumed that the incident current on the cathode side is fully Poissonian but that the transmitted and reflected carrier streams are modified through the current dependence of the transmission probabilities. Our theory takes as the basic noise source the partition noise and treats the associated charge fluctuations self-consistently. To treat the potential fluctuations, we evaluate the off-diagonal elements of a potential operator of the well. In contrast, Ref. 2 does not treat potential fluctuations and Ref. 19 includes self-consistent effects only on the level of probabilities. These works^{2,19} also predict in the PDC range Fano factors lower than $F = 1/2$. Such low Fano factors have been observed in the recent experiment by Kuznetsov *et al.*⁴. However, since in Refs. 2,19 an essential source of noise, the partition noise, which gives raise to the minimal Fano factor $F = 1/2$ in the non-interacting case, is absent, it is perhaps not surprising that lower noise limits are predicted than by our theory.

Below we present a self-consistent, analytical calculation of transport properties of resonant tunneling quantum wells in the limit when the total decay width of the resonant state is lower than all other energy scales of the problem. We consider the zero-temperature case and use the system of units with $\hbar = 1$. We continue to use the expression "shot noise" even in the case when the noise is dominated by interaction. We emphasize, that in this case, we deal not with single independent electrons traversing the conductor, but with a collective response of many electrons. The term "shot noise" underlines here that the basic source of noise is the partition noise, independent of the degree of interaction.

The paper is organized as follows: In Section II we introduce the self-consistency equation and solve it for the average quantities. Sec. III is devoted to the average current. The results of these two sections by themselves are not new, and similar discussion can be found in the literature (see *e.g.* Ref. 12). However, they are necessary for the subsequent calculation of the current-current fluctuations. This calculation is performed in Sec. IV. In Sec. V we present the conclusions and discuss in more detail the conditions of validity of our theory.

II. AVERAGE CHARGE AND POTENTIAL

A. The charge of the well and the self-consistency equation

We consider a quantum well²⁰ extended in the x and y -directions (to be denoted as \perp) with the area \mathcal{A} . The potential profile in the z -direction is shown in Fig. 1. We assume that the longitudinal and the transverse motion of the electrons are separable. The motion in the z -direction is quantized, and there exists a set of resonant levels with energies E_n , $n = 0, 1, \dots$. The transverse motion is described by a continuum of momenta p_\perp . Thus the expression for the total energy (measured from the band bottom of the well) is

$$E_{n,p_\perp} = E_n + p_\perp^2/2m.$$

The density of states in the well can be factorized into longitudinal and transverse parts,

$$\nu(E) = \nu_2 \nu_z(E_z), \quad E = E_z + p_\perp^2/2m.$$

Here $\nu_2 = m/2\pi$ is the two-dimensional density of states (per spin).

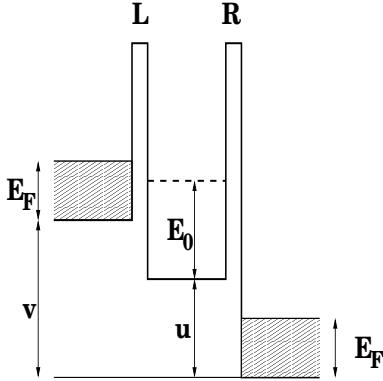


FIG. 1. The potential profile of the quantum well.

For interacting electrons the band bottom of the well $u = eU$ (see Fig. (1)) is not an independent quantity but must be found from a self-consistency equation. In the present work, we account for the interaction by including the energy required to charge the well. We introduce the capacitances C_L and C_R of the left and the right barrier, respectively. The charge allowed in the well by the Coulomb interaction is then determined by these capacitances and the voltage drop across the left barrier $u - v$ and across the right barrier u . Here $v > 0$ is the voltage applied across the double barrier structure. (We assume that the Fermi energies of the left and right contact are equal). Thus the total charge $Q[u]$ in the well is

$$C_L(u - v) + C_R u = eQ[u]. \quad (5)$$

Note that the charge Q is always non-negative, and thus the band bottom either assumes the value $u_e = (C_L + C_R)^{-1} C_L v$ of the empty well, or lies above it.

Throughout this work, we describe scattering at the double barrier in the Breit-Wigner limit. In particular, the longitudinal density of states is

$$\nu_z(E_z) = \frac{1}{2\pi} \sum_n \frac{\Gamma(E_z)}{(E_z - E_n)^2 + \Gamma^2(E_z)/4}. \quad (6)$$

Here we have introduced the total width of a single resonance $\Gamma(E_z) = \Gamma_L(E_z) + \Gamma_R(E_z)$ with $\Gamma_L(E_z)$ and $\Gamma_R(E_z)$ being the partial widths for decay through the left and right barrier, respectively. The Breit-Wigner limit is appropriate in the limit of small tunneling probabilities through the two barriers and provides an excellent description as long as the resonant level is not in the immediate vicinity of the band bottom of any reservoir, $u + E_n = v$.

In the standard application of the Breit-Wigner expression the partial width is independent of energy; for energies E_z close to the resonant state with energy E_n the width is evaluated at the energy of the resonant state, $\Gamma(E_n)$. Here, in order to describe the density of states in the limit where the resonant level approaches the conduction band bottom, we consider the decay widths to be energy dependent. We determine the energy dependence by considering the quantum-mechanical problem of transmission through a single rectangular barrier. We write

$$\begin{aligned} \Gamma_L(E_z) &= a_L E_z^{1/2} (E_z + u - v)^{1/2} \theta(E_z) \theta(E_z + u - v); \\ \Gamma_R(E_z) &= a_R E_z^{1/2} (E_z + u)^{1/2} \theta(E_z) \theta(E_z + u), \end{aligned} \quad (7)$$

where a_L and a_R are dimensionless parameters.

With the density of states as specified above, we can now find the charge $Q[u]$ inside the well. For this purpose, we divide the total longitudinal density of states $\nu_z(E)$ given by Eq. (6) into the partial densities of states of electrons which are incident from the left or the right reservoirs,

$$\nu_z(E_z) = \nu_L(E_z) + \nu_R(E_z).$$

We find²¹

$$\nu_{L,R}(E_z) = \frac{\Gamma_{L,R}(E_z)}{\Gamma(E_z)} \nu_z(E_z). \quad (8)$$

With the distribution functions $f_{L,R}$ of the left and right reservoir and the short-hand notation $E_\perp \equiv p_\perp^2/2m$, we find for the charge of the well

$$Q[u] = e \sum_{p_\perp} \int dE_z \sum_{i=L,R} \nu_i(E_z) f_i(E_z + E_\perp). \quad (9)$$

Eq. (9) gives the total charge in the well in terms of the carriers injected from each reservoir.

To proceed we now specify two additional conditions:

(i) Of all longitudinal energy levels only E_0 is relevant, all others lie too high. In addition, we assume for definiteness $E_0 > E_F$.

(ii) The decay widths Γ_L and Γ_R are much smaller than all other energy scales. In particular, we will re-

place $(\xi^2 + \Gamma^2/4)^{-1}$ by $2\pi\Gamma^{-1}\delta(\xi)$, where appropriate.

Making use of these conditions and replacing the sum over p_\perp by an integral, we obtain

$$Q[u] = \begin{cases} C_e \frac{\Gamma_L(E_0)}{\Gamma(E_0)}(v + E_F - u - E_0), & v - E_0 < u < v - E_0 + E_F, \\ 0, & \text{otherwise.} \end{cases} \quad (10)$$

Here we have introduced the ‘‘quantum capacitance’’ $C_e \equiv e\nu_2\mathcal{A}$ of the two-dimensional electron gas. The dependence of $Q[u]$ on u is shown schematically in Fig. 2 (solid line).

B. Self-consistent calculation of the band bottom u

Equation (5) expresses the band bottom in the well u as a function of the applied voltage v . The equation is cubic and can be solved analytically. However, the resulting expressions are cumbersome and not very transparent. Therefore, we discuss now the behavior of the function $u(v)$ qualitatively, and support the discussion by numerical results (Fig. 2).

The left-hand side of Eq. (5) turns to zero (empty well) for $u = (C_L + C_R)^{-1}C_L v$. The charge is non-zero only between $u = v - E_0$ and $u = v - E_0 + E_F$. With the help of the voltages

$$v_a \equiv \frac{C_L + C_R}{C_R}(E_0 - E_F); \quad v_b \equiv \frac{C_L + C_R}{C_R}E_0,$$

we can distinguish the following four regimes:

I. $0 < v < v_a$ (Fig. 2a). The well is uncharged; the only solution of Eq. (5) is,

$$u(v) = u_e \equiv \frac{C_L}{C_L + C_R}v. \quad (11)$$

II. $v_a < v < v_b$ (Fig. 2b). The well is now charged, but Eq. (5) has still only one solution.

III. $v_b < v < v^*$ (Fig. 2c). For voltages above v_b three solutions emerge; now $u_1(v)$ is given by Eq. (11) and corresponds to the uncharged well, while two others $u_2(v)$ and $u_3(v)$ describe a charged well. The lesser of them, $u_2(v)$, is unstable, and the greater one, $u_3(v)$, is stable. At a certain voltage v^* , which is a complicated function of the parameters of the system, the straight line $e^{-1}[C_L(u - v) + C_R u]$ is a tangent to $Q[u]$. This voltage determines the upper margin for this regime.

IV. $v^* < v$ (Fig. 2d). The well is again uncharged, and the only solution is given by Eq. (11).

The dependence $u[v]$ is illustrated in Fig. 3.

III. AVERAGE CURRENT

To find the current across the quantum well, we start from the general expression for the current density,

$$j = \frac{e}{2\pi\mathcal{A}} \sum_{p_\perp} \int dE_z T(E_z) \times [f_L(E_z + E_\perp) - f_R(E_z + E_\perp)], \quad (12)$$

where $T(E_z)$ is the transmission coefficient, equal to²²

$$T(E_z) = \frac{\Gamma_L(E_z)\Gamma_R(E_z)}{(E_z - E_0)^2 + \Gamma^2(E_z)/4}. \quad (13)$$

Treating Eq. (12) in the same way as previously Eq. (9), we obtain

$$j = \frac{C_e}{\mathcal{A}} \frac{\Gamma_L(E_0)\Gamma_R(E_0)}{\Gamma(E_0)}(v + E_F - u - E_0) \quad (14)$$

for $v < u + E_0 < v + E_F$ and zero otherwise.

This can be easily translated into the current-voltage characteristics, given the known dependence $u(v)$. The current is zero for $v < v_a$ and $v > v^*$. For $v_a < v < v_b$ it is given by Eq. (14), where u is replaced by the only solution $u(v)$. Finally, for $v_b < v < v^*$ the three possible solutions $u(v)$ yield three values for the current for any voltage. One of them is $j = 0$ and corresponds to the uncharged well (the solution $u_1(v)$). Two other branches correspond to the charged well; the stable branch (3 in Fig. 3, due to $u_3(v)$) lies above the unstable one (2). The current-voltage characteristics is shown in Fig. 4 (solid line). The differential resistance jumps from zero to a finite positive value at $v = v_a$ and then decreases with voltage, passing through zero at a certain point. It is negative for voltages close to v^* and turns to $-\infty$ at this point.

In the experiment the system is expected to exhibit a hysteretic behavior (cf. Ref. 12). Upon increasing the voltage, the current follows the upper branch (3 in Fig. 4) until $v = v^*$, and then jumps onto the zero-current branch. Upon decreasing the voltage, the current is zero

until $v = v_b$, and then jumps to a finite value on the branch 3. The unstable branch 2 is not observed. Note that the range of hysteresis $v^* - v_b$ is broader than the range of negative differential resistance.

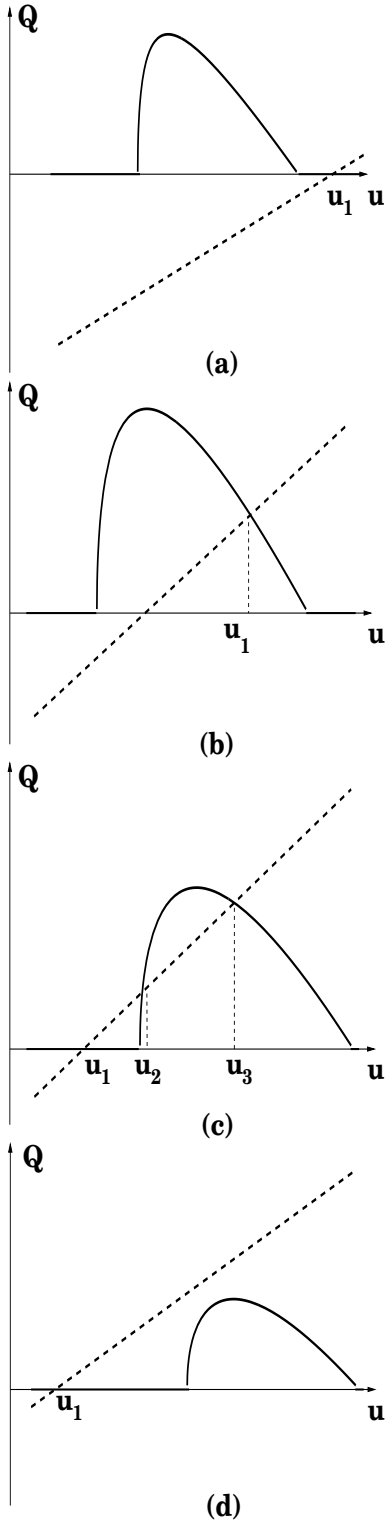


FIG. 2. Solutions of the self-consistency equation (5). The solid line represents the charge $Q[u]$; the dashed line is $e^{-1}[C_L(u-v) + C_R u]$. The position of the vertical axis is arbitrary. The following set of parameters is chosen: $a_L = a_R$; $C_L = C_R = C_e/10$; $E_0 = 3E_F/2$. Voltages are (in units of E_0) 1/3 (a), 1 (b), 7/3 (c), 3 (d). The voltage v^* is equal to 2.70. The solutions are shown as u_i ; in the case (c) there are three solutions, of which u_1 and u_3 are stable, and u_2 is unstable.

The above analysis is valid in the case of low transparency, $\Gamma(E_0) \ll v^* - v_b$. In the opposite case the hysteretic range is smeared, and a broad range of negative differential conductance appears instead. For weak interaction $C_e \ll C_L, C_R$ the width of the hysteretic range is rather small,

$$v^* - v_b = \left(\frac{a_L C_e}{2a_R C_L + C_R} \right)^2 \frac{E_F^2}{E_0},$$

but it increases with the capacitance C_e and eventually must exceed the smearing $\Gamma(E_0)$ of the resonant level.

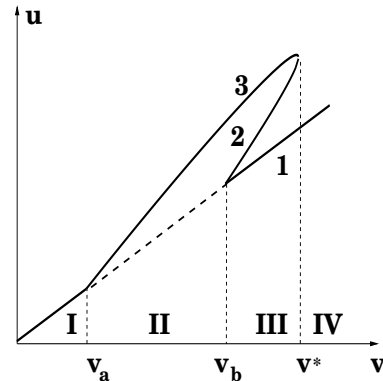


FIG. 3. Dependence $u(v)$ (solid line). Curves 1, 2, and 3 in the regime III correspond to the solutions u_1 , u_2 , and u_3 , respectively. The solution u_2 is unstable. The parameter set is the same as for Fig. 2.

IV. FLUCTUATIONS

A. Charge operator

The fluctuations of the charge, the potential and the current are determined by the off-diagonal elements of these quantities. We must use operator expressions instead of average quantities. Following Ref. 23, we introduce creation and annihilation operators $\hat{a}_\alpha^\dagger(E_z, p_\perp)$ and $\hat{a}_\alpha(E_z, p_\perp)$ of carriers in the reservoir $\alpha = L, R$. The quantum statistical average of bilinear products of these operators is

$$\begin{aligned} \langle \hat{a}_\alpha^\dagger(E_z, p_\perp) \hat{a}_\beta(E'_z, p'_\perp) \rangle &= \delta_{\alpha\beta} \delta_{p_\perp p'_\perp} \\ &\times \delta(E_z - E'_z) f_\alpha(E_z + p_\perp^2/2m). \end{aligned} \quad (15)$$

Here we are interested in the zero-frequency spectral correlations. In this limit the off-diagonal elements of the charge operator can be obtained with the help of off-diagonal density of states elements which in turn can be related to energy derivatives of the scattering matrix. In the presence of a current amplitude incident at contact α and a current amplitude at contact β the off-diagonal density of states element $\nu_{\alpha\beta}$, in terms of scattering matrices $s_{\alpha\beta}$, is^{24,25}

$$\nu_{\alpha\beta}(E_z) = \frac{1}{4\pi i} \sum_{\gamma} \left[s_{\gamma\alpha}^{\dagger} \frac{ds_{\gamma\beta}}{dE_z} - \frac{ds_{\gamma\alpha}^{\dagger}}{dE_z} s_{\gamma\beta} \right]. \quad (16)$$

Using the explicit expressions for the scattering matrices²¹,

$$s_{\alpha\beta} = \exp[i(\phi_{\alpha} + \phi_{\beta})] \left(\delta_{\alpha\beta} - i \frac{\sqrt{\Gamma_{\alpha}\Gamma_{\beta}}}{E_z - E_0 + i\Gamma/2} \right) \quad (17)$$

(with ϕ_{α} being arbitrary phases), and having in mind that the main singularity is generated by the derivative of the denominator in Eq. (17), we easily obtain

$$\nu_{\alpha\beta}(E_z) = \frac{1}{2\pi} \frac{\sqrt{\Gamma_{\alpha}(E_z)\Gamma_{\beta}(E_z)}}{(E_z - E_0)^2 + \Gamma^2(E_z)/4} e^{i(\phi_{\beta} - \phi_{\alpha})}. \quad (18)$$

With the help of these off-diagonal density of states elements the operator of the charge of the well is²⁴

$$\hat{Q}(t) = e \sum_{\alpha\beta} \sum_{p_{\perp}} \int d\omega e^{-i\omega t} \int dE_z \nu_{\alpha\beta}(E_z) \times \hat{a}_{\alpha}^{\dagger}(E_z, p_{\perp}) \hat{a}_{\beta}(E_z + \omega, p_{\perp}). \quad (19)$$

It is straightforward to check that Eq. (19) reproduces the average charge (9). Below we will use the charge operator to find the fluctuations.

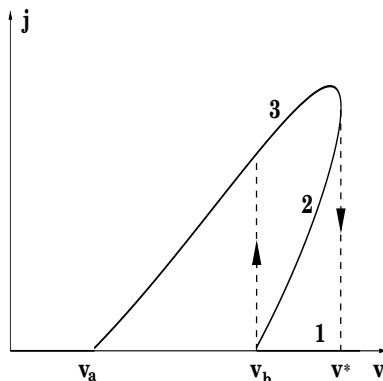


FIG. 4. The current-voltage characteristics $j(v)$ (solid line). The hysteric behavior is shown by dashed lines. The parameter set is the same as for Fig. 2.

B. Band bottom operator

With Q being an operator, the self-consistency equation (5) must be considered as an operator equation. Thus, we are obliged to introduce the band bottom operator \hat{u} , which is a solution of Eq. (5). A similar approach has already been used in Ref. 25. The charge operator \hat{Q} becomes then a superoperator $\hat{Q}[\hat{u}]$. In the following we consider only the voltage range $v_a < v < v^*$, and in case of multiple stable states only the one corresponding to the charged well (denoted $u_3(v)$ in the preceding discussion).

Eq. (5) is non-linear. Instead of trying to find a general solution, we linearize it, writing $\hat{u} = u + \delta\hat{u}$, where u is the solution of Eq. (5) for the average quantities. With the “parameter” of the expansion being $\hat{a}_{\alpha}^{\dagger}\hat{a}_{\beta} - \langle\hat{a}_{\alpha}^{\dagger}\hat{a}_{\beta}\rangle$, we write the charge operator as follows,

$$\begin{aligned} \hat{Q}[\hat{u}] &= \langle Q[u] \rangle + \hat{Q}_1 + \hat{Q}_2, \\ \hat{Q}_1 &= -\frac{C_0[u]}{e} \delta\hat{u}; \quad C_0[u] \equiv -e \frac{\partial \langle Q \rangle}{\partial u}; \\ \hat{Q}_2 &= e \sum_{\alpha\beta} \sum_{p_{\perp}} \int d\omega e^{-i\omega t} \int dE_z \nu_{\alpha\beta}(E_z; u) \\ &\quad \times [\hat{a}_{\alpha}^{\dagger}(E_z, p_{\perp}) \hat{a}_{\beta}(E_z + \omega, p_{\perp}) - \\ &\quad - \langle \hat{a}_{\alpha}^{\dagger}(E_z, p_{\perp}) \hat{a}_{\beta}(E_z + \omega, p_{\perp}) \rangle]. \end{aligned} \quad (20)$$

Here the average charge $\langle Q \rangle$ is given by Eq. (10) and is a function of the average potential u (not of the operator \hat{u}). The capacitance²⁶ $C_0[u]$ determines the charge increment in the well in response to an increment of the potential in the well. It is one of the important response functions which determines the new parameter Λ which eventually enters the Fano factor and was, therefore, mentioned already in the introduction (see Eq. (1), $U = u/e$). On the stable branch (3 in Fig. 3) the “capacitance” C_0 changes sign, and for the voltage v^* it is negative and equal to $-(C_L + C_R)$. The operator \hat{Q}_2 appears as the operator for the bare (unscreened) charge and is a function of the average potential u . For the operator $\delta\hat{u}$ we obtain

$$\delta\hat{u}(t) = \frac{e}{C_L + C_R + C_0[u]} \hat{Q}_2(t). \quad (21)$$

For $v \rightarrow v^*$ this expression diverges. We will show later that this divergence is at the origin of the noise enhancement as the voltage v^* is approached.

C. Current operator

Following Ref. 23, we write the current density operator in the contact α ,

$$\begin{aligned} \hat{j}_{\alpha}(t) &= \frac{e}{2\pi\mathcal{A}} \sum_{\beta\gamma} \sum_{p_{\perp}} \int dE_z dE'_z e^{i(E_z - E'_z)t} A_{\beta\gamma}^{\alpha}(E_z, E'_z) \\ &\quad \times \hat{a}_{\beta}^{\dagger}(E_z, p_{\perp}) \hat{a}_{\gamma}(E'_z, p_{\perp}), \end{aligned} \quad (22)$$

with current matrix elements

$$A_{\beta\gamma}^\alpha(E_z, E'_z) = \delta_{\alpha\beta}\delta_{\alpha\gamma} - s_{\alpha\beta}^\dagger(E_z)s_{\alpha\gamma}(E'_z) \quad (23)$$

which are themselves functions of the operator \hat{u} . Using Eq. (17), we obtain

$$\begin{aligned} A_{LL}^L(E_z, E_z) &= A_{RR}^R(E_z, E_z) = -A_{RR}^L(E_z, E_z) \\ &= -A_{LL}^R(E_z, E_z) = \frac{\Gamma_L(E_z)\Gamma_R(E_z)}{(E_z - E_0)^2 + \Gamma^2/4}. \end{aligned} \quad (24)$$

It is immediately seen that $\langle j_L \rangle = -\langle j_R \rangle$ and the average current $\langle j_L \rangle$ reproduces Eq. (12).

The current operator (22) also must be linearized in $\delta\hat{u}$ in the same manner as we did it for the charge operator. We obtain

$$\begin{aligned} \hat{j}_\alpha[\hat{u}] &= \langle j_\alpha[u] \rangle + \hat{j}_{1\alpha} + \hat{j}_{2\alpha}, \\ \hat{j}_{1\alpha} &= J_\alpha \delta\hat{u}; \quad J_\alpha \equiv \frac{\partial \langle j_\alpha \rangle}{\partial u}; \\ \hat{j}_{2\alpha} &= \frac{e}{2\pi\mathcal{A}} \sum_{\beta\gamma} \sum_{p_\perp} \int dE_z dE'_z e^{-i(E'_z - E_z)t} A_{\beta\gamma}^\alpha(E_z; E'_z) \end{aligned} \quad (25)$$

$$\begin{aligned} &\times \left[\hat{a}_\beta^\dagger(E_z, p_\perp) \hat{a}_\gamma(E'_z, p_\perp) - \right. \\ &\left. - \langle \hat{a}_\beta^\dagger(E_z, p_\perp) \hat{a}_\gamma(E'_z, p_\perp) \rangle \right]. \end{aligned}$$

The current operator $\hat{j}_{1\alpha}$ is proportional to J_α , the increment in current at contact α in response to a potential variation in the well. J_α is the second important response function which enters the Fano factor and has also been mentioned in the introduction (see Eq. (2)). $\hat{j}_{2\alpha}$ is the bare current density and via the current matrix $A_{\beta\gamma}^\alpha$ depends on u (not on \hat{u}). Note that $J_L = -J_R$ and that in the introductory section we have suppressed the contact index and have defined $J \equiv e\mathcal{A}J_L = -e\mathcal{A}J_R$, $U = u/e$.

D. Current-current fluctuations and the Fano factor

Now we are in a position to evaluate the shot noise spectral power $S_{\alpha\beta}$, defined as²³

$$2\pi\delta(\omega + \omega') S_{\alpha\beta}(\omega) = \int dt dt' e^{i\omega t + i\omega' t'} \left[\langle \hat{j}_\alpha(t) \hat{j}_\beta(t') + \hat{j}_\beta(t') \hat{j}_\alpha(t) \rangle - 2 \langle \hat{j}_\alpha(t) \rangle \langle \hat{j}_\beta(t') \rangle \right]. \quad (26)$$

We consider the zero-frequency limit and use the property²³

$$\begin{aligned} &\langle \hat{a}_\alpha^\dagger(E_1, p_\perp) \hat{a}_\beta(E_2, p_\perp) \hat{a}_\gamma^\dagger(E_3, p'_\perp) \hat{a}_\delta(E_4, p'_\perp) \rangle - \langle \hat{a}_\alpha^\dagger(E_1, p_\perp) \hat{a}_\beta(E_2, p_\perp) \rangle \langle \hat{a}_\gamma^\dagger(E_3, p'_\perp) \hat{a}_\delta(E_4, p'_\perp) \rangle \\ &= \delta_{\alpha\delta} \delta_{\beta\gamma} \delta_{p_\perp p'_\perp} \delta(E_1 - E_4) \delta(E_2 - E_3) f_\alpha(E_1 + p_\perp^2/2m) \left[1 - f_\beta(E_2 + p'_\perp^2/2m) \right]. \end{aligned} \quad (27)$$

After simple but tedious algebra where we replace at an intermediate stage $((E_z - E_0)^2 + \Gamma^2(E_z)/4)^{-2}$ by $4\pi\Gamma^{-3}(E_0)\delta(E_z - E_0)$, we obtain $S_{LL} = S_{RR} = -S_{LR} = -S_{RL}$ (thus checking the conservation of current) with

$$\begin{aligned} S_{LL} \equiv S_{LL}(0) &= \frac{2e^2\nu_2}{\mathcal{A}} \frac{\Gamma_L(E_0)\Gamma_R(E_0)}{\Gamma(E_0)^3} \\ &\times (v - u + E_F - E_0) \left\{ \Gamma_L^2(E_0) + \Gamma_R^2(E_0) \right. \\ &+ 2 \frac{e\mathcal{A}J_L}{C_L + C_R + C_0} [\Gamma_R(E_0) - \Gamma_L(E_0)] \\ &\left. + 2 \left(\frac{e\mathcal{A}J_L}{C_L + C_R + C_0} \right)^2 \right\} \end{aligned} \quad (28)$$

for $v_a < v < v^*$ and $S_{LL} = 0$ otherwise.

With the help of the spectral density of the current noise, evaluated on the stable branch of the I-V characteristic, we can find the Fano factor. With the interaction energy

$$\Lambda \equiv \frac{e\mathcal{A}J_L}{C_L + C_R + C_0}, \quad \Gamma_{L,R} \equiv \Gamma_{L,R}(E_0)$$

we find

$$F = \frac{\Gamma_L^2 + \Gamma_R^2 + 2\Lambda[\Gamma_R - \Gamma_L] + 2\Lambda^2}{[\Gamma_L + \Gamma_R]^2}. \quad (29)$$

Eq. (29) is the main result of our work and together with the definitions of J_L and C_0 and with the equation (5) for $u(v)$ (the stable charged branch solution) in an implicit form gives the dependence of the noise power on the applied voltage v . Using Eq. (29) for the Fano factor and the definition of the asymmetry $\Delta\Gamma = (\Gamma_L - \Gamma_R)/2$ gives the Fano factor, Eq. (4), mentioned in the introduction.

The dependence on the Fano factor on the external voltage v is illustrated in an explicit manner in Fig. 5.

There are several important points to comment on.

First, the function $\Lambda(v)$ accommodates the interaction parameter C_e and represents the contribution of interactions to the noise power. For $\Lambda = 0$ (no interaction) we reproduce the free-electron result⁵ $F_0 = (\Gamma_L^2 + \Gamma_R^2)(\Gamma_L + \Gamma_R)^{-2}$, as already discussed in the introduction. Note, however, that due to the energy dependence of the tunneling rates for a symmetric dot, $a_L = a_R$, one has $\Gamma_L < \Gamma_R$, which implies $1/2 < F_0 < 1$.

Furthermore, for $v \rightarrow v^*$ the denominator $C_L + C_R + C_0(v)$ of the function $\Lambda(v)$ quite generally diverges as $(v^* - v)^{-1/2}$, while the function $J_L(v)$ in the numerator stays finite. Consequently, the Fano factor diverges according to $(v^* - v)^{-1}$. This is clearly seen in Fig. 5.

For $v = v_a = C_R^{-1}(C_L + C_R)(E_0 - E_F)$ the Fano factor can be calculated in a closed form. We have

$$C_0(v_a) = C_e \frac{\Gamma_L}{\Gamma_L + \Gamma_R},$$

$$J_L(v_a) = -e\nu_2 \frac{\Gamma_L \Gamma_R}{\Gamma_L + \Gamma_R},$$

which gives

$$\Lambda(v_a) = -\frac{C_e \Gamma_L \Gamma_R}{(C_L + C_R)(\Gamma_L + \Gamma_R) + C_e \Gamma_L} < 0.$$

It is seen that $-\Gamma_R < \Lambda(v_a) < 0$, implying $1/2 < F(v_a) < 1$. Thus, we have described the transition from

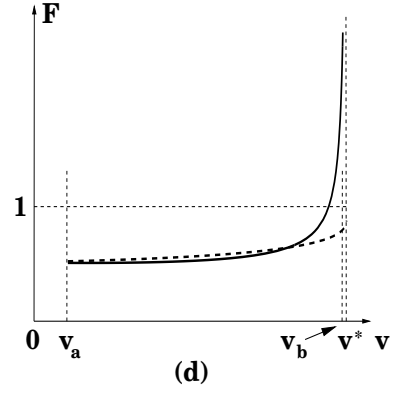
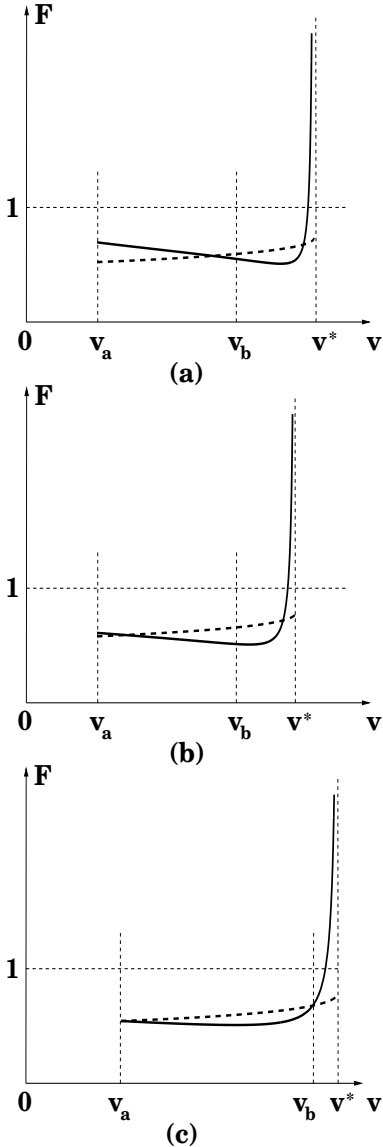


FIG. 5. The full Fano factor F (solid line) and its non-interacting part F_0 (bold dashed line) as a function of applied voltage v . The parameters are chosen as follows: $a_L = a_R$; $C_L = C_R$; (a) $C_e = 10C_L$, $E_0 = 3E_F/2$ (this set corresponds to that of Fig. 2–4); (b) $C_e = 10C_L$, $E_0 = 3E_F$; (c) $C_e = 4C_L$, $E_0 = 2E_F$; (d) $C_e = C_L$, $E_0 = 3E_F/2$. The voltage v^* (in units of E_0) is equal to 2.70 (a), 2.26 (b), 2.14 (c), 2.02 (d).

sub-Poissonian to *super-Poissonian* shot noise. The range of super-Poissonian noise ($F(v) > 1$) lies at voltages close to v^* ; this range is the larger the stronger the interaction is (the parameters C_e/C_L and C_e/C_R grow) and shrinks with increasing distance of the resonance from the equilibrium Fermi level, i. e. with increasing E_F/E_0 . Note that the onset of the super-Poissonian noise (the voltage where $F[v] = 1$) is unrelated to the point of zero differential resistance ($dj/dv = 0$). Of course, these two points may lie quite close to each other. In addition, the quantity J_L changes sign from negative to positive when the voltage approaches v^* . This implies that Λ also changes sign from negative to positive at the same voltage.

Finally, with respect to the role of interactions, two scenarios emerge: To avoid cumbersome expressions, we perform the analysis for the symmetric case $a_L = a_R$, $C_L = C_R$. Then for “weak interactions”,

$$C_e < \tilde{C} \equiv 4C_L \left(\frac{E_0}{E_F} - 1 \right),$$

we have $F(v_a) < F_0(v_a)$. Thus, the curves $F(v)$ and $F_0(v)$ cross each other only once, when $\Lambda(v) = 0$. This means that interactions suppress the shot noise for “low” voltages and enhance it for “high” voltages, eventually driving the noise power to super-Poissonian values for voltages close to v^* . For “strong interactions”, $C_e > \tilde{C}$, we obtain $F(v_a) > F_0(v_a)$, and the curves cross each other twice. In this case, interactions first enhance the shot noise, then suppress it, and then enhance it again. In the limiting case $C_e \gg C_L$ one has $F(v_a) = 1$; then the shot noise starts from the Poissonian value. Fig. 5a and Fig. 5b represent the “strong interaction” scenario. Fig. 5d illustrates the case of “weak interactions”, while Fig. 5c shows the marginal case $C_e = \tilde{C}$, where one has

$$F(v_a) = F_0(v_a).$$

V. CONCLUSIONS

We now discuss the assumptions we made in the course of the derivation of our result, Eq. (4). First, in order to calculate the shot noise, we linearized the charge and current operators in the fluctuations of the band bottom. Close to the voltage v^* , at the linear stability threshold, where the solutions corresponding to the charged well vanish, these fluctuations become large, and the linearization is not justified any more. Since we evaluate only the zero-frequency response, the quantity $\hat{u}^2(t)$ is not amenable to our treatment, and the limits of this approximation can not be determined. We emphasize, that in the crossover region from sub- to super-Poissonian noise our approach is well justified. Thus, our discussion can be used to determine the range of voltages in which super-Poissonian noise can be observed.

To determine the effect of interactions on the Fano factor, we have neglected the finite width of the resonant level in the evaluation of Λ . For comparison with experiment the broadening of the resonant level (finite Γ) should be taken into account. This would smear all the curves; in particular, the noise power at $v = v^*$ would acquire a finite value. Moreover, if the tunneling rate Γ exceeds the hysteresis interval $v^* - v_b$, an extended range of differential resistance will be observed instead of the hysteretic behavior. We believe that is the case in the experiments of Ref. 3. Note also that in our treatment the interactions make the Fano factor discontinuous at $v = v_a$, where it jumps from the non-interacting value⁵ $F_0(v_a)$ to the renormalized one $F(v_a)$. This discontinuity is also healed by the introduction of the finite width of the resonant level.

In our work we have treated a single resonant level. It is clear that wells which permit to fill a number of subbands can be expected to exhibit even richer behavior than indicated in this work. Since interactions play a dominant role in the wide area resonant double barrier structure considered here, it might be interesting to analyze the noise power of a single discrete level in a quantum dot under high bias and ask if in fact a similar behavior results. It would also be interesting to investigate the effect of potential fluctuations not only in the well but also in the accumulation and depletion layers in the cathode and anode. In the terminology of Ref. 16 we have in such a model internal degrees of the well which couple to the cathode. This would modify the current injection into the well (depending on the charge state) and possibly provides a mechanism which can lead to Fano factors smaller than $F = 1/2$.

In conclusion, we investigated current-voltage characteristics and noise power in resonant tunneling quantum wells in the nonlinear regime. We treated the low-transparency case, when the total width Γ , due to tunnel-

ing, is much lower than all other relevant energy scales. (For the evaluation of the interaction effects, we have taken the transmission coefficient as delta-function in energy). The interaction is taken into account via the charge accumulated in the well due to capacitive coupling to the reservoirs. In this regime, we discovered that interactions dramatically affect transport properties of the quantum well. They produce a range of voltages ($v_b < v < v^*$) where the well can be in one of two stable states, which correspond to a charged well and an uncharged well, respectively. For the current-voltage characteristics, this leads to a hysteretic behavior, as shown in Fig. 4. Interaction effects are even more pronounced in the noise power: At low voltages interactions can either suppress or enhance the noise power below or above the shot noise level predicted by a free-electron theory, and at large voltages the noise power diverges as $(v^* - v)^{-1}$ for $v \rightarrow v^*$, and becomes super-Poissonian close to v^* . Both the noise suppression below the non-interacting value^{2,4} and the strong enhancement of the noise to super-Poissonian values^{3,4} have been observed experimentally. We stress that the range of super-Poissonian noise is generally different from the negative differential resistance range, and may extend well outside the hysteresis range (see the example shown in Fig. 5d). We believe that our results provide an explanation of the role of interactions on the shot noise in resonant wells.

Clearly, the interaction effects in the noise power which we have discussed are very interesting. While the search for interaction effects in mesoscopic physics represents a huge effort, there are up to now, at best very few clearly identified signatures for which both experiments and theory agree. A notable exception are of course the Coulomb blockade effects. We emphasize that the effects discussed here, occur in a state which is a far from equilibrium transport state. Resonant tunneling systems have the important advantage that they represent, at least conceptually, a very simple system and thus provide a unique testing ground for both theories and experiments.

ACKNOWLEDGEMENTS

We thank E. E. Mendez and V. V. Kuznetsov who sent us their results prior to publication. The work was supported by the Swiss National Science Foundation.

¹ Y. P. Li, A. Zaslavsky, D. C. Tsui, M. Santos, and M. Shayegan, Phys. Rev. B **41**, 8388 (1990).

² E. R. Brown, IEEE Trans. Electron Devices **39**, 2686 (1992).

³ G. Iannaccone, G. Lombardi, M. Macucci, and B. Pellegrini, Phys. Rev. Lett. **80**, 1054 (1998).

- ⁴ V. V. Kuznetsov, E. E. Mendez, J. D. Bruno, and J. T. Pham, cond-mat/9805311 (unpublished).
- ⁵ L. Y. Chen and C. S. Ting, Phys. Rev. B **43**, 4535 (1991).
- ⁶ V. A. Khlus, Zh. Eksp. Teor. Fiz. **93**, 2179 (1987) [Sov. Phys. – JETP **66**, 1243 (1987)]; G. B. Lesovik, Pis'ma Zh. Eksp. Teor. Fiz. **49**, 513 (1989) [JETP Lett. **49**, 592 (1989)].
- ⁷ M. Büttiker, Phys. Rev. Lett. **65**, 2901 (1990).
- ⁸ M. J. M. de Jong and C. W. J. Beenakker, in: *Mesoscopic Electron Transport*, ed. by L. L. Sohn, L. P. Kouwenhoven, and G. Schön, NATO ASI Series E, Vol. 345 (Kluwer Academic Publishing, Dordrecht, 1997), p. 225.
- ⁹ M. Büttiker, Physica B **175**, 199 (1991).
- ¹⁰ L. Y. Chen and C. S. Ting, Phys. Rev. B **46**, 4714 (1992).
- ¹¹ J. H. Davies, P. Hyldgaard, S. Hershfield, and J. W. Wilkins, Phys. Rev. B **46**, 9620 (1992).
- ¹² A. Levy Yeyati, F. Flores, and E. V. Anda, Phys. Rev. B **47**, 10543 (1993).
- ¹³ J. H. Davies, J. Carlos Egues, and J. W. Wilkins, Phys. Rev. B **52**, 11259 (1995).
- ¹⁴ G. Iannaccone, M. Macucci, and B. Pellegrini, Phys. Rev. B **55**, 4539 (1997).
- ¹⁵ Ø. Lund Bø and Yu. Galperin, J. Phys. Cond. Matter **8**, 3033 (1996).
- ¹⁶ J. Carlos Egues, S. Hershfield, and J. W. Wilkins, Phys. Rev. B **49**, 13517 (1994).
- ¹⁷ E. Pytte and H. Thomas, Phys. Rev. **179**, 431 (1968).
- ¹⁸ M. Büttiker and H. Thomas, Z. Phys. B **33**, 275 (1979). For recent experimental work see K. Hofbeck, J. Grenzer, E. Schomburg, A. A. Ignatov, K. F. Renk, D. G. Pavel'ev, Yu. Koschurinov, B. Melzer, S. Ivanov, S. Schaposchnikov, and P. S. Kop'ev, Phys. Lett. A **218**, 349 (1996); E. Schomburg, T. Blomeier, K. Hofbeck, J. Grenzer, S. Brandl, I. Lingott, A. A. Ignatov, K. F. Renk, D. G. Pavel'ev, Yu. Koschurinov, B. Ya. Melzer, V. M. Ustinov, S. V. Ivanov, A. Zhukov, and P. S. Kop'ev, Phys. Rev. B **58**, (1998) (unpublished).
- ¹⁹ M. M. Jahan and A. F. Anwar, Solid State Electronics **38**, 429 (1998).
- ²⁰ R. Tsu and L. Esaki, Appl. Phys. Lett. **22**, 562 (1973).
- ²¹ T. Christen and M. Büttiker, Europhys. Lett. **35**, 523 (1996). The densities ν_L and ν_R are called there *injectivities*.
- ²² A. D. Stone and P. A. Lee, Phys. Rev. Lett. **54**, 1196 (1985). For the asymmetric and many channel case see M. Büttiker, IBM J. Res. Develop. **32**, 63 (1988).
- ²³ M. Büttiker, Phys. Rev. B **46**, 12485 (1992).
- ²⁴ M. Büttiker, J. Math. Phys. **37**, 4793 (1996).
- ²⁵ M. Pedersen and M. Büttiker, cond-mat/9803306 (unpublished).
- ²⁶ The capacitance $C_0[u]$ plays here the same role as the polarization function of the transport state defined as $\partial\langle Q \rangle = -e\Pi[u]\partial u$. We have $C_0[u] \equiv e^2\Pi[u]$.